ZÁPADOČESKÁ UNIVERZITA V PLZNI

FAKULTA STROJNÍ

KATEDRA ENERGETICKÝCH STROJŮ A ZAŘÍZENÍ

ZÁPADOČESKÁ UNIVERZITA V PLZNI

POWER SYSTEM ENGINEERING, THERMODYNAMICS & FLUID FLOW

2013

JEDNOTLIVÝ PŘÍSPĚVEK ZE SBORNÍKU

evropský sociální fond v ČR

EVROPSKÁ UNIE

MINISTERSTVO ŠKOLSTVÍ, MLÁDEŽE A TĚLOVÝCHOVY

OP Vzdělávání pro konkurenceschopnost

INVESTICE DO ROZVOJE VZDĚLÁVÁNÍ

NUMERICAL SIMULATION OF 2D AND 3D INVISCID AND LAMINAR FLOWS

HUML Jaroslav, KOZEL Karel

The article deals with a numerical simulation of inviscid and viscous (laminar) compressible flows in a GAMM channel, its 3D modification and a DCA 8% cascade. The results are discussed and compared with other similar ones and experiment. A multistage Runge-Kutta method and a Lax-Wendroff scheme (FVM) with Jameson's artificial dissipation were applied on non-orthogonal structured grids.

Keywords: subsonic, transonic, compressible flow, GAMM, DCA cascade, Runge-Kutta

Introduction

The goal of the work is to use and verify the experience and knowledge obtained by the solution of previous, simplier problems of 2D flows for the solution more difficult problems of 2D or 3D flows (e.g. 3D flows around airfoils – a 3D modification of the GAMM channel called *Swept Wing*). Especially then the obtained knowledge of the problems of the inlet boundary conditions that were verified in the previous works have been used for the solution of these and next problems.

1. Mathematical model

The authors have used a system of the Euler equations for a 2D and 3D inviscid compressible flow

$$W_t + F_x + G_y = 0$$

and

$$W_t + F_x + G_y + H_z = 0,$$

where (conservative vectors are written for the 3D case, components containing a velocity w in the direction of axis z are neglected in the 2D case)

$$W = \begin{bmatrix} \rho \\ \rho u \\ \rho v \\ \rho w \\ e \end{bmatrix},\quad F = \begin{bmatrix} \rho u \\ \rho u^2 + p \\ \rho u v \\ \rho u w \\ (e+p)u \end{bmatrix},\quad G = \begin{bmatrix} \rho v \\ \rho u v \\ \rho v^2 + p \\ \rho v w \\ (e+p)v \end{bmatrix},\quad H = \begin{bmatrix} \rho w \\ \rho u w \\ \rho v w \\ \rho w^2 + p \\ (e+p)w \end{bmatrix}.$$

And a system of the Navier-Stokes equations was used for a 2D laminar compressible flow

$$W_t + F_x + G_y = R_x + S_y$$

where

$$R = \left(0, \tau_{xx}, \tau_{xy}, u\tau_{xx} + v\tau_{xy} + \lambda T_x\right)^T,\quad S = \left(0, \tau_{xy}, \tau_{yy}, u\tau_{xy} + v\tau_{yy} + \lambda T_y\right)^T.$$

The systems, whose variables are considered dimensionless, are closed by semi-empirical equations (e.g. Fourier law) and the equation of state in the following form

$$p=(\mu-1)\left[e-\frac{1}{2}\rho\left(u^2+v^2\right)\right],\ \text{alternatively}\ \ p=(\mu-1)\left[e-\frac{1}{2}\rho\left(u^2+v^2+w^2\right)\right].$$

2. Numerical method and schemes

The numerical solution of all the flows considered was obtained by the multistage Runge-Kutta method (RK, here is written for the 3D inviscid case)

$$\begin{aligned}
&Res\ W_{i,j,k}^{(r)}=\frac{1}{\mu\left(D_{i,j,k}\right)}\sum\left(\tilde{F},\tilde{G},\tilde{H}\right)_{i,j,k,l}\cdot\vec{n}_{i,j,k,l}^{0}\,\Delta S_{i,j,k,l},\\
&W_{i,j,k}^{(0)}=W_{i,j,k}^{n},\\
&W_{i,j,k}^{(r+1)}=W_{i,j,k}^{(0)}-\alpha_r\,\Delta t Res\ W_{i,j,k}^{(r)}+AD\left(W_{i,j,k}^{n}\right),\ \ r=0,1,2\\
&W_{i,j,k}^{n=1}=W_{i,j,k}^{(3)}\\
&\alpha_{0,1}=0.5,\alpha_2=1
\end{aligned}$$

and Lax-Wendroff scheme (a predictor-corrector form by Richtmyer is shown for the 2D inviscid cases, LW)

$$\begin{aligned}
W_{i,j}^{n+1/2}&=W_{i,j}^{n}-\frac{1}{2}\frac{\Delta t}{\mu\left(D_{i,j}\right)}\sum\left(\tilde{F}_{i,j,l}^{n}\Delta y_l-\tilde{G}_{i,j,l}^{n}\Delta x_l\right)+\frac{\varepsilon}{4}\sum\left(W_l^n-W_{i,j}^n\right),\\
W_{i,j}^{n+1}&=W_{i,j}^{n}-\frac{1}{2}\frac{\Delta t}{\mu\left(D_{i,j}\right)}\sum\left(\tilde{F}_{i,j,l}^{n+1/2}\Delta y_l-\tilde{G}_{i,j,l}^{n+1/2}\Delta x_l\right)+AD\left(W_{i,j}^n\right)
\end{aligned}$$

of the finite volume methods on non-orthogonal structured grids of the quadrangular (2D) and hexahedral (3D) cells.

Each scheme was extended by including Jameson's artificial dissipation (here is written for the 2D cases, a 3D version is simply extended taking the third components into consideration) to improve the stability of the method

$$AD\left(W_{ij}^n\right)=C_1\psi_1\left(W_{i-1j}^n-2W_{ij}^n+W_{i+1j}^n\right)+C_2\psi_2\left(W_{ij-1}^n-2W_{ij}^n+W_{ij+1}^n\right)$$

where

$$\psi_1=\frac{|p_{i-1j}^n-2p_{ij}^n+p_{i+1j}^n|}{|p_{i-1j}^n|+|p_{ij}^n|+|p_{i+1j}^n|},\ \ \psi_2=\frac{|p_{ij-1}^n-2p_{ij}^n+p_{ij+1}^n|}{|p_{ij-1}^n|+|p_{ij}^n|+|p_{ij+1}^n|}.$$

3. Formulation of the problems

The authors took in account the GAMM channel, 3D extension of the GAMM channel that was called by the authors *Swept Wing* (a relative thickness of the *wing* was changed between 4% and 10%) and the DCA 8% cascade. The outlines of all the computational domains are shown in **Figs. 1 – 3.** An inlet and outlet are always situated on the left and the right hand side of the domain respectively. Other outlines or surfaces mean solid walls or free walls – parts of boundary where periodicity condition was applied.

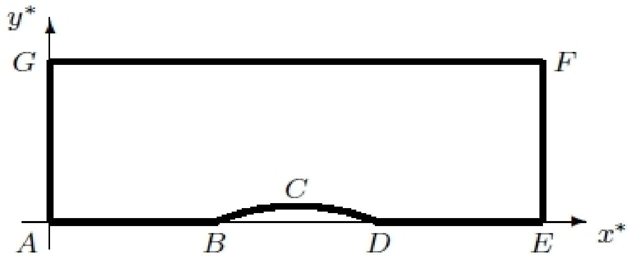

$A = (0, 0)$
$B = (1, 0)$
$C = (1.5, 0.1)$
$D = (2, 0)$
$E = (3, 0)$
$F = (3, 1)$
$G = (0, 1)$

Fig. 1: GAMM channel

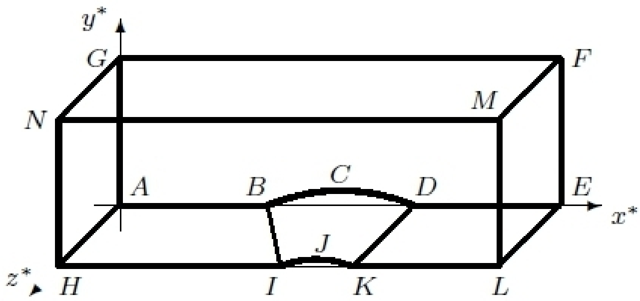

$A = (0, 0, 0)$	$H = (0, 0, 1)$
$B = (1, 0, 0)$	$I = (1.5, 0, 1)$
$C = (1.5, 0.1, 0)$	$J = (1.75, 0.04, 1)$
$D = (2, 0, 0)$	$K = (2, 0, 1)$
$E = (3, 0, 0)$	$L = (3, 0, 1)$
$F = (3, 1, 0)$	$M = (3, 1, 1)$
$G = (0, 1, 0)$	$N = (0, 1, 1)$

Fig. 2: 3D extension of the GAMM channel, called *Swept Wing*

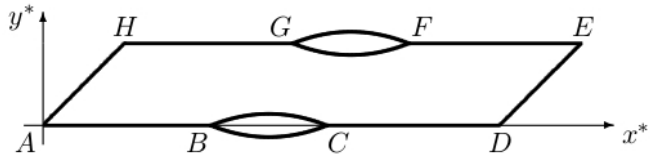

$A = (0, 0)$	$E = (4 + \frac{\sqrt{2}}{2}, \frac{\sqrt{2}}{2})$
$B = (1.5, 0)$	$F = (2.5 + \frac{\sqrt{2}}{2}, \frac{\sqrt{2}}{2})$
$C = (2.5, 0)$	$G = (1.5 + \frac{\sqrt{2}}{2}, \frac{\sqrt{2}}{2})$
$D = (4, 0)$	$H = (\frac{\sqrt{2}}{2}, \frac{\sqrt{2}}{2})$

Fig. 3: DCA 8% cascade

3.1 Boundary Conditions

Inlet: $\rho_1 = 1, u_1 = M_1 \cos\alpha, v_1 = M_1 \sin\alpha, w_1 = 0, p_1$ was extrapolated from the flow field and e_1 was calculated using the equation of state, where α is angle of attack that is zero for flows in GAMM channel and *Swept Wing*.

Outlet: p_2 was prescribed, ρ_2, u_2, v_2, w_2 were extrapolated from the flow field and e_2 was calculated using the equation of state,

The boundary conditions on the solid wall and the periodicity conditions were implemented by using virtual cells adjoined from outside of the computational domain and values of the variables inside of them were prescribed to obtain the desired effect.

Solid wall: velocity components were prescribed so that a sum of velocity vectors equals to zero $u = v = w = 0$ (a viscous flow) or equals to zero in their tangential component $(u, v, w)\vec{n} = 0$ (an inviscid flow).

Periodicity: a value of the variable in a cell at the bottom part of boundary corresponds to a value in a cell from the flow field near the top part boundary.

Initial conditions were prescribed to comply with the inlet conditions.

4. Numerical results

The authors used two types of non-orthogonal structured grids of quadrilateral or hexahedral cells, the mesh of first type had a constant resolution and in the second case the mesh was thickened along the walls, i.e. a convenient refinement of the mesh near the solid walls was made for the better detection of viscosity influence (see **Figs. 4 – 5**).

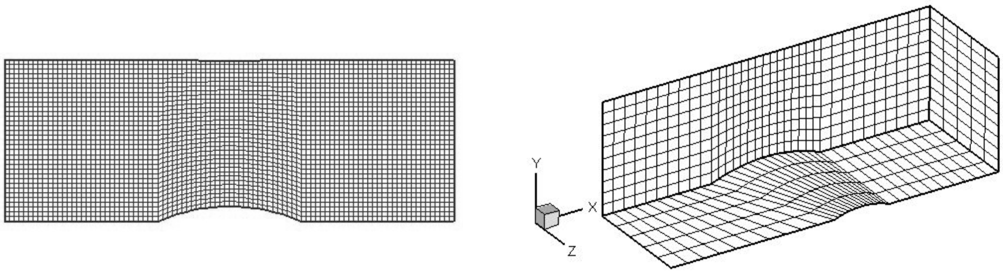

Fig. 4: Sketches of the grids for the GAMM channel (left) and the *Swept Wing* (right) – the used resolutions 150x50 cells and 110x30x10 cells respectively

Fig. 5: Sketches of two grids for the DCA 8% cascade – the used resolutions 130x50 cells (inviscid flow, left) and 170x120 cells (laminar flow, right)

The authors took in account several values of inlet Mach and Reynolds numbers, and angles of attack to obtain numerical results of a subsonic and transonic flow, which were comparable with the experimental data and other similar numerical solution for the verification and satisfaction of the use of a software developed by the authors that used the multistage Runge-Kutta method and/or Lax-Wendroff scheme in the Richtmyer's predictor-corrector form.

In the **Figs. 6 – 9**, you can see some results for 2D inviscid and laminar compressible transonic flows in the GAMM channel at the inlet Mach number $M_1=0.675$ and $M_1=0.675, R_1=10^6$ in the laminar case. The largest maximum Mach number was reached (ca. $M_{max}=1.4$), when LW scheme was used. But otherwise the results obtained by LW and RK are comparable both each other and with the results by J. Fürst [5] that were chosen for the comparison.

The Mach number isolines for the 3D inviscid compressible flow are shown in the **Figs. 10** and **11**. Smaller values of Mach number were obtained in the comparison with the results by J. Holman [5] and the Zierep singularity was not reached due to a smaller grid resolution.

Inviscid and laminar compressible transonic flows in the DCA 8% cascede, that are presented in the **Figs. 12 – 17**, were compared to results by P. Pořízková – **Figs. 15** and **17** – and with the experiment (carried out by R. Dvořák at the Institute of Thermodynamics AS CZ, [1]) – **Fig. 13**. A good agreement was found both with the results by P. Pořízková and with the experimets.

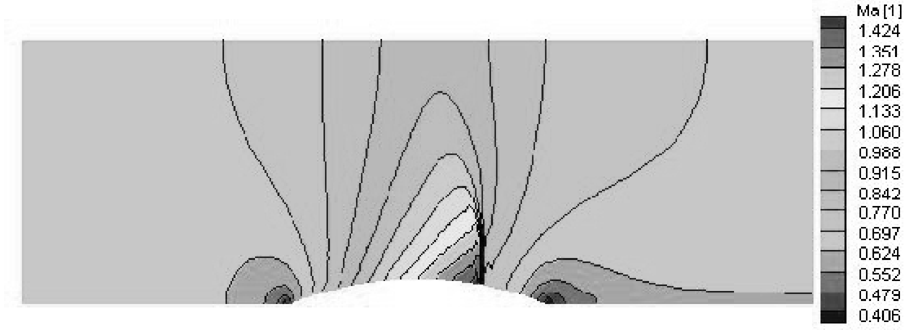

Fig. 6: Inviscid compressible flow in the GAMM channel, LW scheme, Mach number isolines, $M_1 = 0.675$

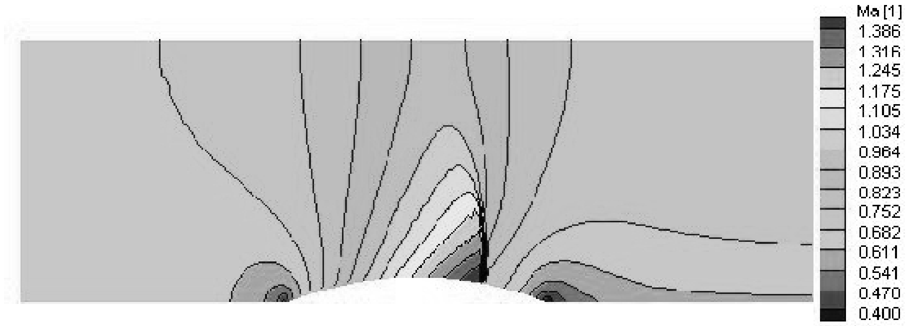

Fig. 7: Inviscid compressible flow in the GAMM channel, RK scheme, Mach number isolines, $M_1 = 0.675$

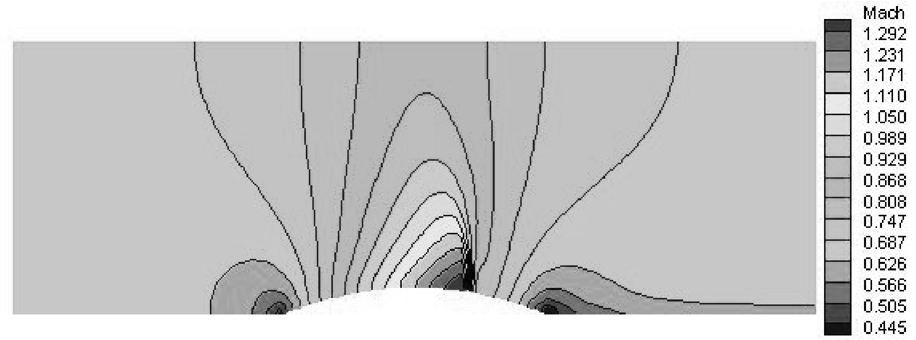

Fig. 8: Inviscid compressible flow in the GAMM channel, WLSQR scheme, Mach number isolines, $M_1 = 0.675$, **author: Fürst [5]**

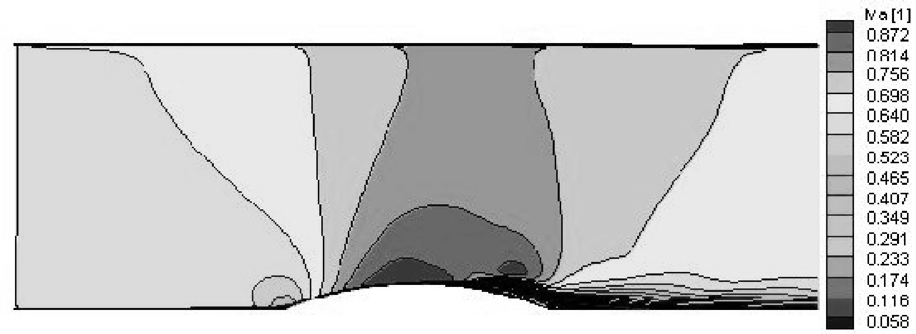

Fig. 9: Laminar compressible flow in the GAMM channel, LW scheme, Mach number isolines, $M_1 = 0.65, R_1 = 10^6$

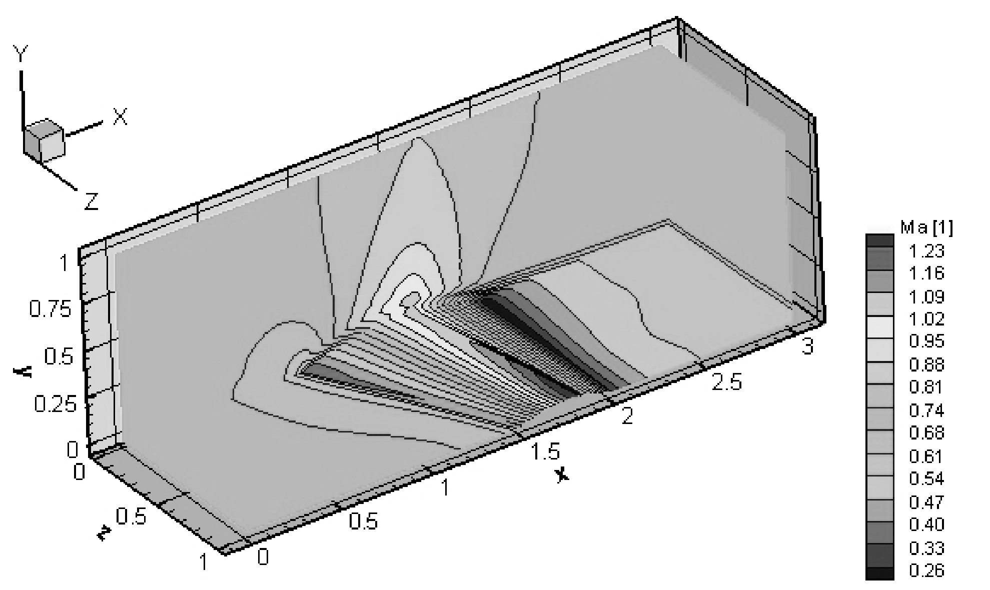

Fig. 10: Inviscid compressible flow in the *Swept Wing*, RK scheme, Mach number isolines, $M_1 = 0.675$

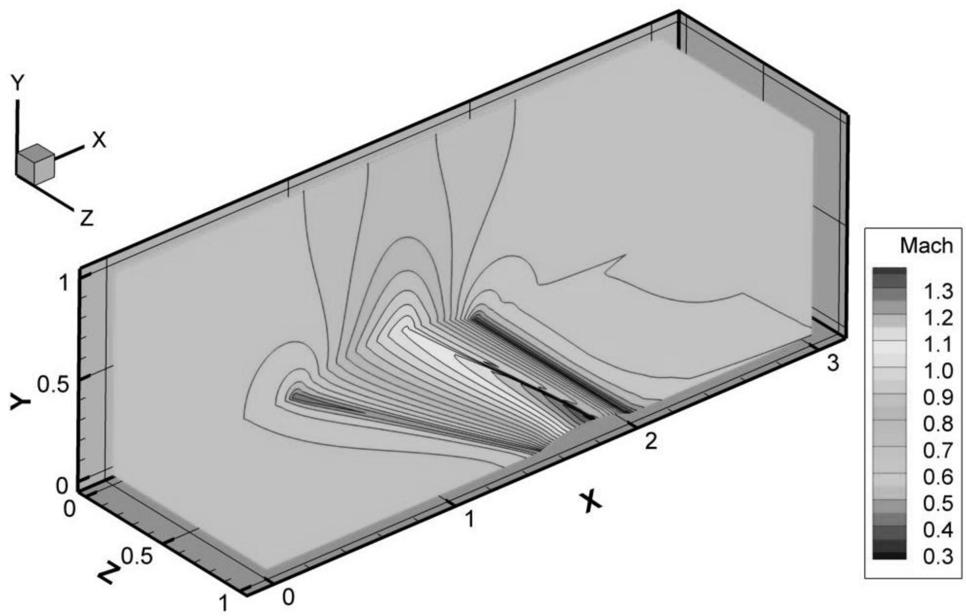

Fig. 11: Inviscid compressible flow in the *Swept Wing* (mesh: 130x30x30 cells), WLSQR scheme, Mach number isolines, $M_1 = 0.675$, **author: Holman [5]**

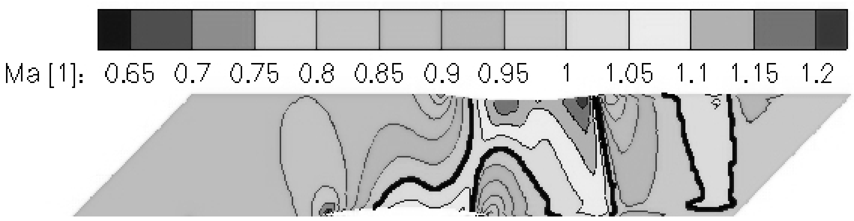

Fig. 12: Inviscid compressible flow in the DCA 8% cascade, RK scheme, Mach number isolines, $M_1 = 0.92$, $\alpha = 2°$

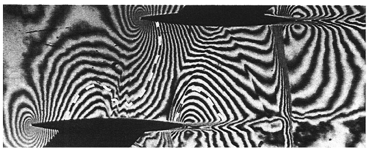

Fig. 13: Compressible flow in the DCA 8% cascade, experiment IT CAS CR, Mach number isolines, $M_1 = 0.863, \alpha = 0°$, **author: R. Dvořák [1]**

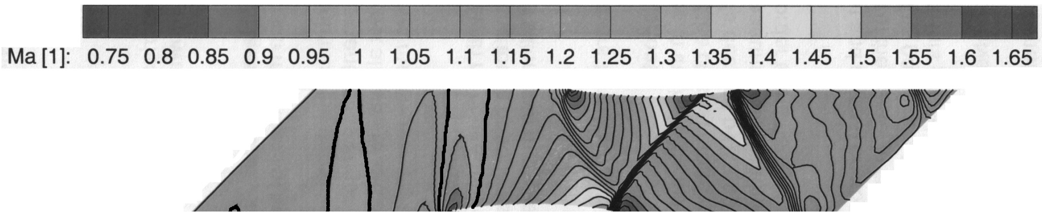

Fig. 14: Inviscid compressible flow in the DCA 8% cascade, RK scheme, Mach number isolines, $M_1 = 1.12,\ \alpha = 0.5°$

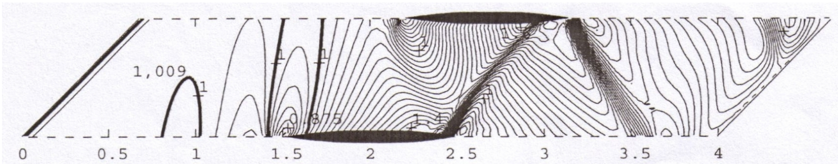

Fig. 15: Inviscid compressible flow in the DCA 8% cascade (mesh: 150x30 cells), a composite scheme, Mach number isolines, $M_1 = 1.12, \alpha = 0°$, **author: P. Pořízková [6]**

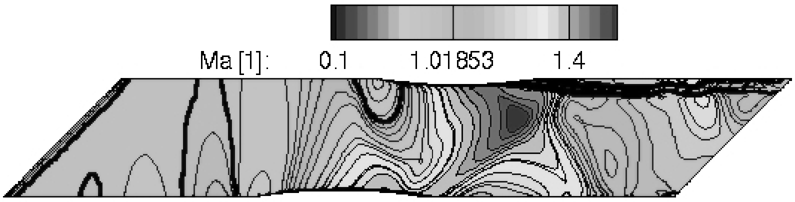

Fig. 16:
Laminar compressible flow in the DCA 8% cascade, RK scheme, Mach number isolines, $M_1 = 1.1, Re = 2.1 \cdot 10^{6,} \alpha = 0°$

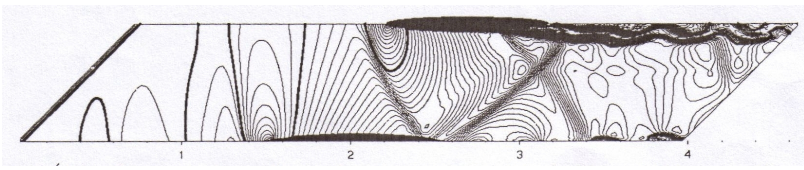

Fig. 17: Laminar compressible flow in the DCA 8% cascade (mesh: 150x30 cells), MacCormack scheme, Mach number isolines, $M_1 = 1.1, Re = 2.1 \cdot 10^{6,} \alpha = 0°$, **author: P. Pořízková [6]**

Conclusion

The work presents some numerical results of a 2D and 3D subsonic and transonic flow of an inviscid and viscous (laminar) compressible fluid in the GAMM channel and its 3D modification Swept Wing, and in the DCA 8% cascade that were achieved by using authors' software with the implemented FVM multistage Runge-Kutta method and the added Jameson's artificial dissipation. The numerical results shows the good agreement with other numerical results (e.g. J. Holman [5] or P. Pořízková [6]) and experimental results carried out at the Institute of Thermodynamics AS CZ ([1]).

Literature

[1] DVOŘÁK, R. Transsonické proudění, Academia, Praha, pp. 162-172, 1986

[2] DVOŘÁK, R.; KOZEL, K. Matematické modelování v aerodynamice, Vydavatelství ČVUT, Praha, 1996

[3] FOŘT, J.; KOZEL, K.; LOUDA, P.; FÜRST, J. Numerické metody řešení problémů proudění 3, Vydavatelství ČVUT, Praha, 2004

[4] KOZEL, K.; FÜRST, J. Numerické metody řešení problémů proudění 1, Vydavatelství ČVUT, Praha, 2001

[5] HOLMAN, J.; FÜRST, J. Comparision of High Order Methods for Transonic Inviscid Flows. Colloquium Fluid Dynamics 2008, Institute of Thermomechanics, AS CR, v. v. i., Prague, pp. 11-12, October 22-24, 2008

[6] POŘÍZKOVÁ, P. Numerical Solution of Compressible Flows Using Finite Volume Method. PhD Dissertation CTU in Prague, Faculty of Mechanical Engineering, CTU in Prague, 2009 [in Czech]

Acknowledgment

This work was partly supported by grants No. P101/10/1329, P101/12/1271 and 13-005-22S of the Grant Agency of the Czech Republic, grant No. IAA200760801 of the Grant Agency of the Academy of Science of the Czech Republic and grant No. SGS 10/243/OHK2/3T/12 of the Student Grant Competition of Czech Technical University in Prague.

Ing. **HUML Jaroslav**, Czech Technical University in Prague, Faculty of Mechanical Engineering, Department of Technical Mathematics,
Karlovo nám. 13, CZ-121 35 Prague, +420 224 357 430, jar.huml@centrum.cz
prof. RNDr. DrSc. **KOZEL Karel**, Czech Technical University in Prague, Faculty of Mechanical Engineering, Department of Technical Mathematics,
Karlovo nám. 13, CZ-121 35 Prague, +420 224 357 301, karel.kozel@fs.cvut.cz